Journal of Materials Chemistry A

Pore Environment Engineering in Metal-Organic Frameworks for Efficient Ethane/Ethylene Separation

Journal:	*Journal of Materials Chemistry A*
Manuscript ID	TA-ART-03-2019-002822.R1
Article Type:	Paper
Date Submitted by the Author:	17-Apr-2019
Complete List of Authors:	Wang, Xun; South China University of Technology, Chemistry and Chemical Engineering Niu, Zheng; University of South Florida, Department of Chemistry Al-Enizi, Abdullah; King Saud University, Chemistry Nafady, Ayman; King Saud University, Chemistry Department; College of Science, King Saud University, Chemistry Wu, Yufang; South China University of Technology, Chemistry and Chemical Engineering Aguila, Briana; University of South Florida, Department of Chemistry Verma, Gaurav; University of South Florida, Chemistry Wojtas, Lukasz; University of South Florida, Department of Chemistry Chen, Yu-Sheng; University of Chicago Advanced Photon Source,, ChemMatCARS Li, Zhong; South China University of Technology, School of Chemistry and Chemical Engineering Ma, Shengqian; University of South Florida, Department of Chemistry

Journal Name

ARTICLE

Pore Environment Engineering in Metal-Organic Frameworks for Efficient Ethane/Ethylene Separation

Received 00th January 20xx,
Accepted 00th January 20xx

DOI: 10.1039/x0xx00000x

www.rsc.org/

Xun Wang, †[a,b] Zheng Niu, †[b] Abdullah M. Al-Enizi,[c] Ayman Nafady, [c,d] Yufang Wu,[a] Briana Aguila,[b] Gaurav Verma,[b] Lukasz Wojtas,[b] Yu-Sheng Chen,[e] Zhong Li,*[a] Shengqian Ma*[b]

Selective adsorption of trace amount of C_2H_6 from bulk C_2H_4 is a significantly important and extemely challenging task in industry, which requires an adsorbent with specific pore properties. Herein, we describe a strategy for adjusting the pore environment of metal-organic frameworks (MOFs) by introducing different amounts of methyl groups in the channel to enhance the guest-host interaction between C_2H_6 and the framework. To prove this concept, 2,3,5,6-tetramethylterephthalic acid (TMBDC) was delebertely added into a microporous MOF, Ni(BDC)(DABCO)$_{0.5}$, affording a series of mixed-ligand materials, Ni(BDC)$_{1-x}$(TMBDC)$_x$(DABCO)$_{0.5}$ (x = 0, 0.2, 0.45, 0.71, 1) having different pore environments. Significantly, these mixed-ligand materials demonstrated improved performance in terms of the adsorption capacity of C_2H_6 and C_2H_4 with an unprecedented C_2H_6 uptake of 2.21 mmol/g for Ni(TMBDC)(DABCO)$_{0.5}$ at 0.0625 bar and 298 K. With the best theoretical C_2H_6/C_2H_4 selectivity predicted by IAST, the Ni(TMBDC)(DABCO)$_{0.5}$ exhibited effective separation of C_2H_6/C_2H_4 (1/15, v/v) and great recyclability in five consecutive adsorption/desorption cycles throughout the breakthrough experiment.

Introduction

As the most important raw material for manufacturing plastics, ethylene (C_2H_4) is primarily obtained via steam cracking and thermal decomposition of ethane (C_2H_6).[1] The separation of C_2H_4/C_2H_6 mixtures becomes a challenging issue at the large scale because of their similar molecular sizes and volatilities.[2] In industry, the ethylene is separated from ethane through cryogenic distillation at low temperature (183 – 258 K) and high pressure (7 – 28 bar), making it an extremely energy exhaustive process.[1, 2] Therefore, separation approaches that have low cost and energy-saving are highly desirable in industry. Among several new technologies, adsorptive separation has attracted extensive interest due to its operational simplicity and the ability to afford high product purity.[3-5] The cornerstone of this promising technology is a solid adsorbent with specific properties.

Over the past few decades, metal-organic frameworks (MOFs)[6-13] have been explored as one kind of highly efficient solid adsorbent for gas storage and separation because of their high surface areas, adjustable pore environments, and designable framework structures.[14-25] Research on the separation of ethylene/ethane using MOFs with open metal sites has been widely reported, in which high ethylene uptake capacities and C_2H_4/C_2H_6 selectivities have been achieved.[26-32] Furthermore, π-complexation adsorbents,[33] such as Cu(I)-based sorbents[34,35] and Ag(I)-based sorbents,[36-39] were developed since these materials can form π-complexation with the carbon-carbon double bonds of C_2H_4, resulting in higher ethylene capacities and C_2H_4 selectivities over C_2H_6. Virtually, these materials preferentially adsorb C_2H_4 in C_2H_4/C_2H_6 mixtures owing to the interactions between the open metal sites of the MOFs and C_2H_4 or formation of π-complexation. Such a behavior is expected to consume more energy during desorption because these interactions are stronger than the traditional physisorption.

Practically, the ethylene concentration in the cracked gas feed is much higher than that of ethane (C_2H_4:C_2H_6 = 15:1, v/v) and consequently large amounts of adsorbents are required, giving rise to a larger packed-bed column. In this context, it is strategically essential to develop ethane-selective adsorbents for preferential adsorption of trace amount of C_2H_6 from bulk C_2H_4. Nevertheless, this class of materials have rarely been reported and most of them exhibited poor C_2H_6/C_2H_4 adsorption capacities and/or separation performances.[41-45] Importantly, simulation and experimental results revealed that C_2H_6 interacts more strongly with the material’s framework than C_2H_4 owing to the fact that C_2H_6 has more C-H bonds.[41, 43-46] Inspired by these endeavors, we propose a strategy for constructing a binding environment in MOFs that favors C_2H_6 over

---

[a] *School of Chemistry and Chemical Engineering, South China University of Technology, Guangzhou, 510640, China; E-mail: cezhli@scut.edu.cn*
[b] *Department of Chemistry, University of South Florida, 4202 East Fowler Avenue, Tampa, Florida, 33620, United States, Fax: +1 813-974-3203; Tel: +1 813-974-5217; E-mail: sqma@usf.edu*
[c] *Department of Chemistry, College of Science, King Saud University, Riyadh 11451, Saudi Arabia*
[d] *Chemistry Department, Faculty of Science, Sohag University, Sohag 82524, Egypt*
[e] *ChemMatCARS, Center for Advanced Radiation Sources, The University of Chicago, 9700 South Cass Avenue, Argonne, Illinois 60439, United States*

† These authors contributed equally to this work.

Electronic Supplementary Information (ESI) available: Experimental details, TGA curves, ^{1}H NMR data and single-crystal data. CCDC 1879219. For ESI and crystallographic data in CIF or other electronic format. See DOI: 10.1039/x0xx00000x

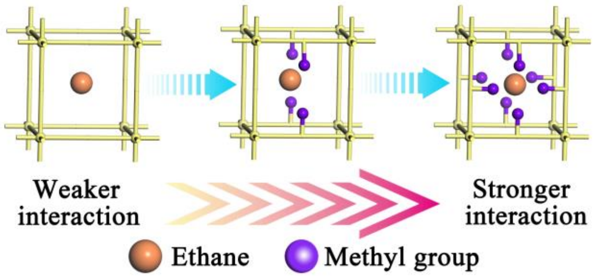

Scheme 1. Schematic illustration of methyl group functionalization in MOF pore to enhance the interaction toward ethane molecule

C_2H_4,through adjusting the guest-host interaction between the pores and C_2H_6 molecules. as illustrated in Scheme 1.

To prove the above concept, we employed a MOF, $Ni(BDC)(DABCO)_{0.5}$,[41, 47-48] (BDC = 1,4-terephthalic acid, DABCO = 1,4-diazabicyclo[2.2.2]octane) as a prototype host material. The methyl group functionalized pores were constructed by introducing different amounts of the TMBDC ligand (TMBDC = 2,3,5,6-tetramethylterephthalic acid) into the framework of $Ni(BDC)(DABCO)_{0.5}$ through a mixed-ligand strategy, affording a series of MOFs, $Ni(BDC)_{1-x}(TMBDC)_x(DABCO)_{0.5}$ (x = 0, 0.2, 0.45, 0.71, 1). The obtained MOFs retained a similar framework, yet exhibited varying C_2H_6/C_2H_4 adsorption performances with change in the mole ratio of TMBDC/BDC. The selectivity of C_2H_6/C_2H_4 based on ideal adsorbed solution theory (IAST) using the single component experimental adsorption isotherms illustrated that the introduction of methyl group into a MOF can effectively enhance the C_2H_6/C_2H_4 separation performance. The designed breakthrough experiments confirmed the IAST calculated results, whereas the adsorption/desorption cycling tests implied the robustness and excellent recyclability of the material.

Experimental

Chemicals

All chemical reagents were purchased from commercial sources (Sigma-Aldrich, Alfa, Fisher, Acros, TCI et.al.) and used without further purification. 2,3,5,6-tetramethylterephthalic acid (TMBDC) was synthesized according to a reported procedure in the literature with some modification (ESI). [49]

Synthesis of $Ni(BDC)_{1-x}(TMBDC)_x(DABCO)_{0.5}$ (x = 0, 0.2, 0.45, 0.71, 1)

General procedure: a 20 mL vial was charged with $Ni(NO_3)_2{\cdot}6H_2O$ (0.093g, 0.32 mmol), DABCO (0.018g, 0.16 mmol), BDC ligands (TMBDC and/or BDC) and 8 mL DMF. After vigorous stirring, one drop of HNO_3 was added. The mixture was sonicated to get a clear solution and then heated at 120 °C for 48 h to afford green crystals. The crystals were collected by filtration and soaked in DMF to remove any residual reactants and then ethanol to exchange the DMF. The obtained $Ni(BDC)_{1-x}(TMBDC)_x(DABCO)_{0.5}$ was kept in ethanol until used. The exact ratio of TMBDC/BDC was determined by ^1H NMR after decomposing the MOFs using HCl solution (ESI, Fig. S5 – S9)

Synthesis of $Ni(BDC)_{0.8}(TMBDC)_{0.2}(DABCO)_{0.5}$: a 20 mL vial was fikled with $Ni(NO_3)_2{\cdot}6H_2O$ (0.093 g, 0.32 mmol), DABCO (0.018 g, 0.16 mmol), TMBDC (0.014 g, 0.06 mmol), BDC (0.04 g, 0.24 mmol) and 8 mL DMF. After heated up to 120 °C for 48 h and purified with DMF and ethanol, the $Ni(BDC)_{0.8}(TMBDC)_{0.2}(DABCO)_{0.5}$ was obtained. (yield: 86% based on DABCO). Elemental Analysis for $C_{11.8}H_{13.6}NO_4Ni$, Anal. Calcd. (%) C, 48.47; H, 4.66; N, 4.66. Found: C, 48.57; H, 4.78; N, 4.56. FTIR (cm^{-1}): 2959 (br), 1613 (m), 1511 (s), 1382 (s), 1229 (w), 1055 (m), 1022 (m).

Synthesis of $Ni(BDC)_{0.55}(TMBDC)_{0.45}(DABCO)_{0.5}$: a 20 mL vial was filled with $Ni(NO_3)_2{\cdot}6H_2O$ (0.093 g, 0.32 mmol), DABCO (0.018 g, 0.16 mmol), TMBDC (0.034 g, 0.15 mmol), BDC (0.025 g, 0.15 mmol) and 8 mL DMF. After heated up to 120 °C for 48 h and purified with DMF and ethanol, the $Ni(BDC)_{0.55}(TMBDC)_{0.45}(DABCO)_{0.5}$ was obtained. (yield: 80% based on DABCO). Elemental Analysis for $C_{12.8}H_{15.6}NO_4Ni$, Anal. Calcd. (%) C, 50.17; H, 5.10; N, 4.57. Found: C, 49.87; H, 5.46; N, 4.46. FTIR (cm^{-1}): 2933 (br), 1603 (m), 1548 (w), 1392 (s), 1230 (s), 1053 (m), 1016 (m).

Synthesis of $Ni(BDC)_{0.29}(TMBDC)_{0.71}(DABCO)_{0.5}$: a 20 mL vial was filed with $Ni(NO_3)_2{\cdot}6H_2O$ (0.093 g, 0.32 mmol), DABCO (0.018 g, 0.16 mmol), TMBDC (0.054 g, 0.24 mmol), BDC (0.01 g, 0.06 mmol) and 8 mL DMF. After heated up to 120 °C for 48 h and purified with DMF and ethanol, the $Ni(BDC)_{0.29}(TMBDC)_{0.71}(DABCO)_{0.5}$ was obtained. (yield: 73% based on DABCO). Elemental Analysis for $C_{13.84}H_{17.68}NO_4Ni$, Anal. Calcd. (%) C, 51.78; H, 5.51; N, 4.36. Found: C, 51.53; H, 5.90; N, 4.29. FTIR (cm^{-1}): 2929 (br), 1601 (m), 1538 (m), 1441 (s), 1376 (s), 1235 (s), 1061 (m), 1016 (m).

Synthesis of $Ni(TMBDC)(DABCO)_{0.5}$: a 20 mL vial was filled with $Ni(NO_3)_2{\cdot}6H_2O$ (0.093g, 0.32 mmol), DABCO (0.018g, 0.16 mmol), TMBDC (0.067 g, 0.3 mmol) and 8 mL DMF. After heated up to 120 °C for 48 h and purified with DMF and ethanol, the $Ni(TMBDC)(DABCO)_{0.5}$ was obtained. (yield: 68% based on DABCO). Elemental Analysis for $C_{15}H_{20}NO_4Ni$, Anal. Calcd. (%) C, 53.41; H, 5.93; N, 4.15. Found: C, 53.16; H, 6.28; N, 4.19. FTIR (cm^{-1}): 2943 (br), 1603 (m), 1596 (s), 1445 (s), 1376 (s), 1230 (s), 1057 (m), 1010 (m).

Synthesis of $Ni(BDC)(DABCO)_{0.5}$: For comparison, $Ni(BDC)(DABCO)_{0.5}$ was prepared according to procedures described elsewhere.[41, 47-48]

Characterization

The N_2 adsorption-desorption isotherms were measured at 77 K using a liquid N_2 bath. The surface area was calculated using the Brunauer-Emmett-Teller equation in the range P/P_0 = 0.05 – 0.35, while the pore size distribution was calculated by the DFT method. All samples were degassed at 120 °C for 6 h before analysis. Powder X-ray diffraction (PXRD) were collected on a Bruker AXS D8 Advance using Cu Kα (λ=1.5406 Å) radiation. The FT-IR data were recorded on a PerkinElmer Spectrum Two. TGA curves were obtained using NETZSCH STA 449F3 Simultaneous Thermal Analyzer (NETZSCH, Germany). ^1H NMR spectra were performed on a UnityInova 400 Spectrometer (400 MHz).

Gas adsorption isotherms

The C_2H_6 and C_2H_4 adsorption isotherms were collected on a 3 Flex Surface Characterization Analyzer (Micromeritics, USA). Before each measurement, the samples were degassed at 120 °C under vacuum for 6 h.

Breakthrough experiments

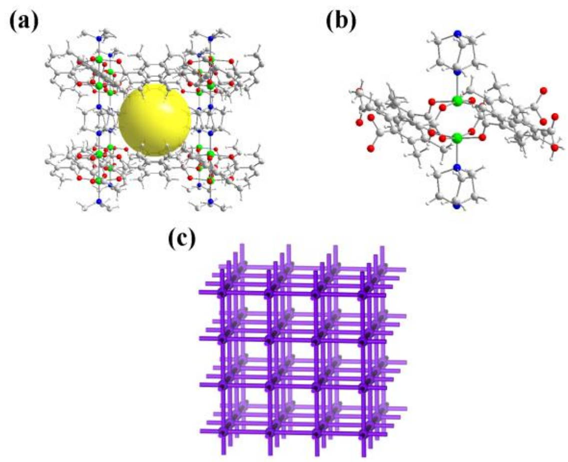

Fig. 1 (a) The primary cavity of Ni(TMBDC)(DABCO)$_{0.5}$; (b)The connection of one nickel paddlewheel and linkers; (c) ***pcu*** topology of Ni(TMBDC)(DABCO)$_{0.5}$ (green, nickel; grey, carbon; blue, nitrogen; red, oxygen; white, hydrogen)

The breakthrough curves of the gas mixture C_2H_6/C_2H_4 (1:15, v/v) were collected on a self-assembly experimental apparatus (Fig. S2). Breakthrough experiments were carried out at 298 K on a gas chromatography apparatus (GC-9560, Shanghai Huaai), equipped with a 2 m long Al_2O_3-packed column with an FID detector. Typically, ~ 200 mg pre-degassed sample was packed into a stainless steel column with inner dimension of Φ6 × 275 mm. The carrier gas was N_2 having a flow rate of 45 mL/min, and the flow rate of C_2H_6/C_2H_4 gas mixture was controlled at 1 mL/min by a mass flow controller (FMA-A200, America). For the consecutive adsorption/desorption cycling tests, the sample packed column was regenerated by purging He at a rate of 30 mL/min at 100 °C for 20 min. After that the gas flow was switched to the C_2H_6/C_2H_4 mixture for the next cycle.

Results and discussion

Characterization of the materials

Solvothermal reaction of 1,4-terephthalic acid (H_2BDC), 2,3,5,6-tetramethylterephthalic acid (TMBDC), 1,4-Diazabicyclo[2.2.2]octane (DABCO) with $Ni(NO_3)_2{\cdot}6H_2O$ in DMF at 120 °C yielded green rod-shaped crystals of Ni(BDC)$_{1-x}$(TMBDC)$_x$(DABCO)$_{0.5}$ (x = 0.2, 0.45, 0.71, 1). The single crystal X-ray diffraction measurement was employed to analyze the structures of the MOFs, and the results revealed that all mixed-ligand samples crystallized in the *P*4/*mmm* space group (Fig. 1a). The structure of Ni(TMBDC)(DABCO)$_{0.5}$ was presented and discussed, since all of them are isostructural. As shown in Figure 1, each nickel paddlewheel is connected with four linear linkers of TMBDC^{2-} to form two-dimensional layers, while the DABCO molecules coordinate at the vertex of the nickel paddlewheels as the pillar to bridge the layers, thus affording the 3D framework (Fig. 1b). Assuming the nickel paddlewheel to be the 6-connected nodes and the ligands as linkers, the Ni(TMBDC)(DABCO)$_{0.5}$ displays a 6-coodinated network with the topology of ***pcu*** (Fig 1c). The primary cavity of Ni(BDC)1-x(TMBDC)x(DABCO)$_{0.5}$ (x = 0.2, 0.45, 0.71, 1) is constructed by eight nickel paddlewheels, eight BDC^{2-} ligands, and four DABCO pillared ligands, exhibiting a cubic shaped cavity suitable to fit a sphere with a diameter of 6.5 – 8.7 Å, which increased along with the decrease of the TMBDC/BDC ratio.

Table 1 BET surface areas and pore volumes of Ni(BDC)$_{1-x}$(TMBDC)$_x$(DABCO)$_{0.5}$ (x = 0, 0.2, 0.45, 0.71, 1)

Materials	BET surface area (m^2/g)	Pore volume (cm^3/g)
Ni(BDC)(DABCO)$_{0.5}$	2050	0.80
Ni(BDC)$_{0.8}$(TMBDC)$_{0.2}$(DABCO)$_{0.5}$	1556	0.63
Ni(BDC)$_{0.55}$(TMBDC)$_{0.45}$(DABCO)$_{0.5}$	1294	0.53
Ni(BDC)$_{0.29}$(TMBDC)$_{0.71}$(DABCO)$_{0.5}$	1084	0.45
Ni(TMBDC)(DABCO)$_{0.5}$	894	0.39

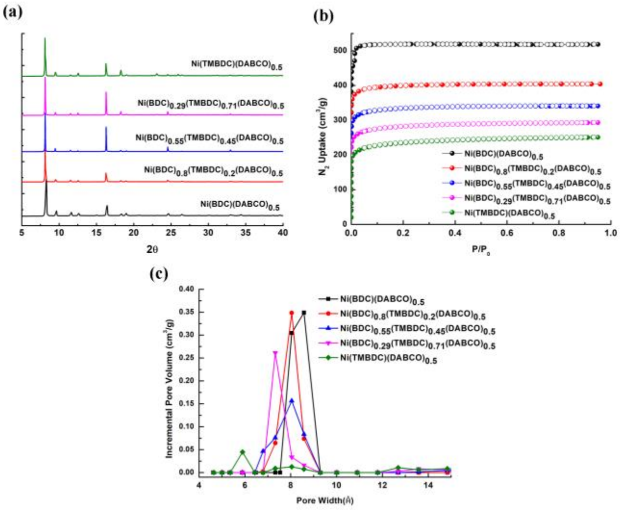

Fig. 2 (a) PXRD patterns, (b) N_2 adsorption-desorption isotherms at 77 K and (c) Pore size distributions of Ni(BDC)1-x(TMBDC)x(DABCO)0.5 (x = 0, 0.2, 0.45, 0.71, 1).

Phase purity of the five materials was confirmed by PXRD studies. As shown in Fig. 2a, the series of materials show high crystallinity and purity. The PXRD patterns of Ni(BDC)(DABCO)$_{0.5}$ are in good agreement with those reported in literatures. [37, 44-46] The Ni(BDC)$_{1-x}$(TMBDC)$_x$(DABCO)$_{0.5}$ (x = 0.2, 0.45, 0.71, 1) retained the same XRD patterns as that of Ni(BDC)(DABCO)$_{0.5}$, implying that the introduction of the TMBDC ligand did not interrupt the crystal phase purity. Thermal stability of Ni(BDC)$_{1-x}$(TMBDC)$_x$(DABCO)$_{0.5}$ (x = 0, 0.2, 0.45, 0.71, 1) was studied by thermogravimetric analysis. All TGA curves exhibited the negligible weight loss before 400 °C and great loss (~65%) after that temperature, which indicated Ni(BDC)$_{1-x}$(TMBDC)$_x$(DABCO)$_{0.5}$ (x = 0, 0.2, 0.45, 0.71, 1) were thermally stable up to 400 °C. (Fig. S2)

Nitrogen adsorption-desorption isotherms at 77 K were used to investigate the porosity of Ni(BDC)$_{1-x}$(TMBDC)$_x$(DABCO)$_{0.5}$ (x = 0, 0.2, 0.45, 0.71, 1). As shown in Fig. 2b, all five materials exhibit typical type-I sorption behaviors, suggesting the microporous structure in their frameworks. With the increase of the TMBDC/BDC ratio, the BET surface area and pore volume of Ni(BDC)$_{1-x}$(TMBDC)$_x$(DABCO)$_{0.5}$ (x = 0, 0.2, 0.45, 0.71, 1) decreases from 2050 m^2/g and 0.80 cm^3/g for Ni(BDC)(DABCO)$_{0.5}$ to 894 m^2/g and 0.39 cm^3/g for

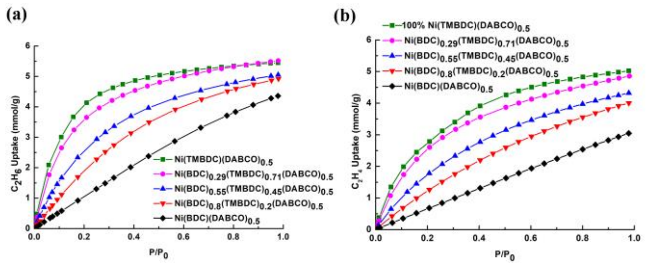

Fig. 3 (a) C_2H_6 and (b) C_2H_4 adsorption isotherms of $Ni(BDC)_{1-x}(TMBDC)_x(DABCO)_{0.5}$ (x = 0, 0.2, 0.45, 0.71, 1) at 298 K.

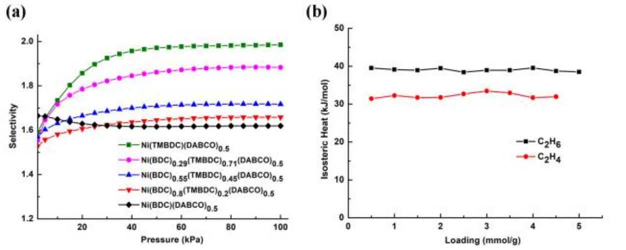

Fig. 4 (a) IAST selectivities of C_2H_6/C_2H_4 (1:15) on $Ni(BDC)_{1-x}(TMBDC)_x(DABCO)_{0.5}$ (x = 0, 0.2, 0.45, 0.71, 1) and (b) Isosteric heats of C_2H_6 and C_2H_4 adsorption on $Ni(TMBDC)(DABCO)_{0.5}$ at 298 K.

$Ni(TMBDC)(DABCO)_{0.5}$, respectively (Table 1). The decrease of both BET surface area and accessible pore volume can be ascribed to the increased number of methyl groups in the framework (Table 1).

Pore size distribution analysis calculated by the density functional theory method (DFT) further confirmed the methyl group occupation in the pores. The results showed that with the increase of the TMBDC/BDC ratio, the main pore size distribution is shifted from ~8.3 Å for $Ni(BDC)(DABCO)_{0.5}$ to ~5.9 Å for 100% $Ni(TMBDC)(DABCO)_{0.5}$.

Consequently, we have judiciously tuned the pore size and pore environment of the pristine $Ni(BDC)(DABCO)_{0.5}$ by introducing the TMBDC ligand into the framework. Through altering the TMBDC/BDC ratio, mixed-ligand materials, $Ni(BDC)_{1-x}(TMBDC)_x(DABCO)_{0.5}$ (x = 0, 0.2, 0.45, 0.71, 1) were successfully synthesized, which is anticipated to influence the adsorption and separation performances of C_2H_6 and C_2H_4 to obtain the desirable C_2H_6/C_2H_4 separation selectivity.

The success of constructing methyl group functionalized pores in the MOFs promoted us to investigate the C_2H_6 and C_2H_4 adsorption performance of $Ni(BDC)_{1-x}(TMBDC)_x(DABCO)_{0.5}$ (x = 0, 0.2, 0.45, 0.71, 1). Single component adsorption isotherms of both C_2H_6 and C_2H_4 (Fig. 3, Fig. S3-S9) were measured at 273 K, 298 K and 308 K. As shown in Fig. 3, all of the $Ni(BDC)_{1-x}(TMBDC)_x(DABCO)_{0.5}$ (x = 0, 0.2, 0.45, 0.71, 1) exhibited preferential adsorption of C_2H_6 over C_2H_4. The equilibrium uptake of C_2H_6 and C_2H_4 for $Ni(BDC)(DABCO)_{0.5}$ can reach 4.36 mmol/g and 3.04 mmol/g at 1 bar, respectively. However, the C_2H_6 and C_2H_4 uptake amounts at the low pressure region (0 –0.3 bar) are not high, which are insufficient to address the challenging issue of the industrial separation of C_2H_6 and C_2H_4.

When the concentration of TMBDC ligand increases, the $Ni(BDC)_{1-x}(TMBDC)_x(DABCO)_{0.5}$ (x = 0.2, 0.45, 0.71, 1) takes up an increasing amount of both ethane and ethylene at 1 bar as well as the low pressure region (0 – 0.3 bar). The equilibrium uptake of C_2H_6 and C_2H_4 for $Ni(TMBDC)(DABCO)_{0.5}$ reached 5.45 mmol/g and 5.02 mmol/g at 1 bar, respectively, which are comparable with the previously reported values of other materials.[27-28, 45, 54-55] However, the high C_2H_6 uptakes in the low pressure region make these materials promising for the challenging separation of trace amount of C_2H_6 from bulk C_2H_4. Given the low concentration of ethane (C_2H_6:C_2H_4 = 1:15, v/v) in the industrial cracked gas feed, the gas uptake at 0.0625 bar (P/P_0 = 0.0625) should be given more attention. As shown in Fig. 3(a), $Ni(TMBDC)(DABCO)_{0.5}$ exhibits an unprecedented C_2H_6 uptake of 2.21 mmol/g at 0.0625 bar, which is higher than 1.47 mmol/g (35 cm^3/g) for MAF-49,[42] 2 mmol/g for $Fe_2(dobdc)$ (318 K),[27] and 0.8 mmol/g for Cu-BTC (295 K).[54] The higher equilibrium uptake and low-pressure uptake of C_2H_6 and C_2H_4 for $Ni(BDC)_{1-x}(TMBDC)_x(DABCO)_{0.5}$ (x = 0.2, 0.45, 0.71, 1) should be ascribed to the introduction of the TMBDC ligand. In principle, as the ratio of TMBDC/BDC increases, the amount of methyl groups from the TMBDC ligand increases, which leads to a stronger interaction toward the gas molecules. C_2H_6 molecules, which have more C-H bonds, are expected to induce stronger interaction with the methyl groups in the MOF than C_2H_4, thereby leading to more preferential adsorption of C_2H_6 in $Ni(BDC)_{1-x}(TMBDC)_x(DABCO)_{0.5}$ (x = 0.2, 0.45, 0.71, 1).

In order to assess the potential of $Ni(BDC)_{1-x}(TMBDC)_x(DABCO)_{0.5}$ (x = 0.2, 0.45, 0.71, 1) for C_2H_6/C_2H_4 separation, ideal adsorbed solution theory (IAST) was used to predict the C_2H_6/C_2H_4 (1:15 v/v) selectivity for all $Ni(BDC)_{1-x}(TMBDC)_x(DABCO)_{0.5}$ (x = 0, 0.2, 0.45, 0.71, 1). Before IAST calculation, C_2H_6 and C_2H_4 adsorption isotherms at 298 K were fitted by dual-site Langmuir-Freundlich (DSLF) model (ESI). As shown in Fig. 4a, the IAST selectivity of pristine $Ni(BDC)(DABCO)_{0.5}$ is 1.619 at 298 K and 100 kPa. As the ratio of TMBDC/BDC is increased, the selectivity of $Ni(BDC)_{1-x}(TMBDC)_x(DABCO)_{0.5}$ (x = 0.2, 0.45, 0.71, 1) increases and reaches up to 1.985 for $Ni(TMBDC)(DABCO)_{0.5}$ at 100 kPa, indicating that it exhibits the best performance for C_2H_6/C_2H_4 separation among these five materials. The interaction between gas molecules and the host framework was evaluated by isosteric heat, Q_{st}, which is calculated by the Clausius-Clapeyron equation (ESI). The obtained Q_{st} of C_2H_6 is slightly higher than that of C_2H_4, further confirming the preferential adsorption of $Ni(TMBDC)(DABCO)_{0.5}$ toward C_2H_6. Additionally, the Q_{st} values of C_2H_6 in $Ni(TMBDC)(DABCO)_{0.5}$ are ~39 kJ/mol, which are higher than the reported values including those of $Ni(BDC)(DABCO)_{0.5}$,[41] IRMOF-8,[42] and MAF-3,[42] illustrating a strong guest-host interaction between the framework of $Ni(TMBDC)(DABCO)_{0.5}$ and C_2H_6 molecules. Based on the outstanding IAST calculation results, $Ni(TMBDC)(DABCO)_{0.5}$ was chosen for further investigations.

To explore the dynamic separation of $Ni(TMBDC)(DABCO)_{0.5}$ for the C_2H_6/C_2H_4 mixture, a breakthrough experiment was undertaken, in which the simulated cracked gas feed of C_2H_6/C_2H_4 (1/15, v/v) was used. As shown in Fig. 5a, a clean and sharp separation of C_2H_6 and C_2H_4 was observed. The initial outlet effluent gas contains only C_2H_4 with high purity (>99.9%), indicating the efficient separation for the C_2H_6/C_2H_4 mixture when $Ni(TMBDC)(DABCO)_{0.5}$ is used as the adsorbent in the packed column. The recycle test of $Ni(TMBDC)(DABCO)_{0.5}$ was evaluated in the breakthrough apparatus. Fig. 5b shows the breakthrough curves of five consecutive adsorption-desorption cycles in a column packed with

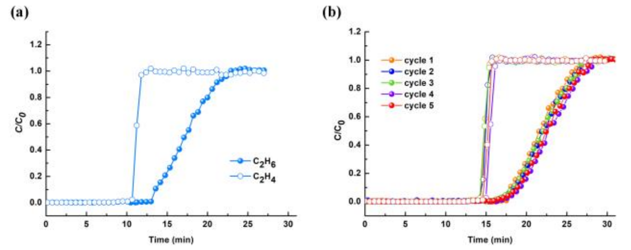

Fig. 5 Breakthrough curves of C_2H_6/C_2H_4 (1:15) in a column packed with Ni(TMBDC)(DABCO)$_{0.5}$ at 298 K (a) in a single run; (b) five consecutive adsorption-desorption cycles.

Ni(TMBDC)(DABCO)$_{0.5}$. In each cycle, the material was regenerated completely within 20 min, showing remarkable recyclability and enhanced stability in the capacity. It should be noted that the Ni(TMBDC)(DABCO)$_{0.5}$ packed column was regenerated without vacuuming, making it feasible for industrial applications.

Conclusions

In summary, a series of Ni(BDC)$_{1-x}$(TMBDC)$_x$(DABCO)$_{0.5}$ (x = 0.2, 0.45, 0.71, 1) with controllable methyl group functionalized pores have been successfully constructed for C_2H_6/C_2H_4 separation. The series of MOFs exhibit similar frameworks but different pore environments. Owing to the adjustment of the methyl groups in the framework, Ni(BDC)$_{1-x}$(TMBDC)$_x$(DABCO)$_{0.5}$ (x =0, 0.2, 0.45, 0.71, 1) shows different guest-host interactions toward C_2H_6 and C_2H_4 than the pristine material, leading to a different adsorption capacity of both C_2H_6 and C_2H_4. Containing more C-H bonds, the adsorption of C_2H_6 is highly favoured in these mixed-ligand materials and an unprecedented C_2H_6 capacity of 2.21 mmol/g at 0.0625 bar was obtained for Ni(TMBDC)(DABCO)$_{0.5}$. With the best IAST selectivity of 1.985 and high Qst of 35 kJ/mol for C_2H_6, Ni(TMBDC)(DABCO)$_{0.5}$ was selected for the breakthrough experiment and recyclability test, which showed great potential for C_2H_6/C_2H_4 (1:15, v/v) separation. Significantly, this pore environment engineering approach is most likely to facilitate the design of other novel MOF materials for other important gas separations.

Conflicts of interest

There are no conflicts to declare

Author contribution

XW, ZL, and SM conceived the research and designed the experiments; XW and ZN conducted the experiments of MOF synthesis and gas sorption measurements; GV, LW, and YSC performed the SCXRD studies; all the authors participate the data discussion and writing of the manuscript.

Acknowledgements

The authors acknowledge the China Scholarship Council (201606150020), Key Program of National Natural Science Foundation of China (No. 21436005), the Guangdong Province Science and Technology Project (No. 2016A020221006), the United States National Science Foundation (DMR-1352065) and the University of South Florida for financial support of this work. Single crystal diffraction data were collected at Argonne National Laboratory, Advanced Photon Source, Beamline 15-ID-B of ChemMatCARS, which is principally supported by the Divisions of Chemistry (CHE) and Materials Research (DMR), National Science Foundation, under grant number NSF/CHE-1346572. The use of the PILATUS3 X CdTe 1M detector is supported by the National Science Foundation under the grant number NSF/DMR-1531283. Use of the Advanced Photon Source, an Office of Science User Facility operated for the U.S. Department of Energy (DOE) Office of Science by Argonne National Laboratory, was supported by the U.S. DOE under Contract No. DE-AC02-06CH11357. The authors also extend their appreciation to the Distinguished Scientist Fellowship Program (DSFP) at King Saud University for partial funding of this work.

Notes and references

‡ Footnotes relating to the main text should appear here. These might include comments relevant to but not central to the matter under discussion, limited experimental and spectral data, and crystallographic data.

1 S. Matar & L. F. Hatch, Chemistry of Petrochemical Processes 2nd edition (Gulf Publishing Company, 2001).
2 T. Ren, M. Patel, K. Blok, *Energy.*, 2006, **31**, 425
3 D. S. Sholl, R. P. Lively, *Nature.*, 2016, **532**, 435
4 D. M. Ruthven, S. C. Reyes, *Micropor. Mesopor. Mat.*, 2007, **104**, 59
5 H. Jȁrvelin, J. R. Fair, *Ind. Eng. Chem. Res.*, 1993, **32**, 2201
6 P. Kumar, K. –H. Kim, E. E. Kwon, J. E. Szulejko, *J. Mater. Chem. A*, 2016, **4**, 345
7 H. –C. Zhou, J. R. Long, O. M. Yaghi, *Chem. Rev.*, 2012, **112**, 673
8 H. Furukawa, K. E. Cordova, M. O'Keeffe, O. M. Yaghi, *Science*, 2013, **341**, 1230444
9 H.-C. Zhou, S. Kitagawa, *Chem. Soc. Rev.*, 2014, **43**, 5415
10 J. Jiang, Y. Zhao and O. M. Yaghi, *J. Am. Chem. Soc.*, 2016, **138**, 3255
11 F. ZareKarizi, M. Joharian, A. Morsali, *J. Mater. Chem. A*, 2018, **6**, 19288
12 Y. Cui, B. Li, B. Chen, G. Qian, *Acc. Chem. Res.*, 2016, **49**, 483
13 B. Li, H. –M. Wen, G. Qian, B. Chen et al., *Adv. Mater.*, 2016, **28**, 8819
14 M. P. Suh, H. J. Park, T.K. Prasad, D.W. Lim, *Chem. Rev.*, 2012, **112**, 782
15 X. Zhao, Y. Wang, D-S. Li, X. Bu, P. Feng, *Adv. Mater.*, 2018, **30**, 1705189
16 A. Cadiau, K. Adil, P. M. Bhatt, Y. Belmabkhout, M. Eddaoudi, *Science*, 2016, **353**, 137
17 J. –R. Li, J. Sculley, H. –C, Zhou, *Chem. Rev.*, 2012, **112**, 869
18 K. Sumida, D. L. Rogow, J. A. Mason, J. R. Long, et al., *Chem. Rev.*, 2012, **112**, 724
19 Y. He, W. Zhou, G. Qian, B. Chen et al., *Chem. Soc. Rev.*, 2014, **43**, 5657
20 Y. Peng, J. T. Hupp, O. K. Farha, T. Yildirim, *J. Am. Chem. Soc.*, 2013, **135**, 11887

21 J. Jiang, H. Furukawa, Y. –B. Zhang, O. M. Yaghi, *J. Am. Chem. Soc.*, 2016, **138**, 10244
22 S. Xiang, Y. He, Z. Zhang, R. Krishna. B. Chen et al., *Nat. Commun.*, 2012, **3**, 954
23 S. Ma, H. –C. Zhou, *Chem. Commun.*, 2010, **46**, 44
24 T. Islamoglu, S. Goswami, O. K. Farha, J. T. Hupp, *Acc. Chem. Res.*, 2017, **50**, 805
25 K. Adil, Y. Belmabkhout. M. Eddaoudi et al., *Chem. Soc. Rev.*, 2017, **46**, 3402
26 Z. Bao, G. Chang, H. Xing, R. Krishna, Q. Ren, B. Chen et al., *Energy Environ. Sci.*, 2016, **9**, 3612
27 E. D. Bloch, W. L. Queen, R. Krishna, J. M. Zadrozny, C. M. Brown, J. R. Long, *Science*, 2012, **335**, 1606
28 R.-B. Lin, L. Li, H.-L. Zhou, H. Wu, C. He, J. Li, W. Zhou, B. Chen et al., *Nat. Mater.*, 2018, **17**, 1128
29 Z. R. Herm, E. D. Bloch, J. R. Long, *Chem. Mater.*, 2014, **26**, 323
30 S. J. Gerier, J. A. Mason, E. D. Bloch, W. L. Queen, M. R. Hudson, C. M. Brown, J. R. Long, *Chem. Sci.*, 2013, **4**, 2054
31 Y. He, R. Krishna, B. Chen, *Energy Environ. Sci.*, 2012, **5**, 9107
32 V.F.D. Martins, A. M. Ribeiro, A. E. Rodrigues et al., *Sep. Purif. Technol.*, 2015, **149**, 445
33 D. J. Safarik, R. B. Eldridge, *Ind. Eng. Chem. Res.*, 1998, **37**, 2571
34 G. Chang, Z. Bao, Q. Ren, S. Deng, Z. Zhang, B. Su, H. Xing, Y. Yang, *RSC Adv.*, 2014, **4**, 20230
35 F. Gao, Y. Wang, X. Wang, S. Wang, *Adsorption.*, 2016, **22**, 1013
36 G. Chang, Y. Su, Q. Ren, Z. Bao, B. Chen et al, *Chem. Commun.*, 2015, **51**, 2859
37 B. Li, Y. Zhang, R. Krishna, K. Yao, Y. Han, Z. Wu, D. Ma, Z. Shi, S. Ma, et al. *J. Am. Chem. Soc.*, 2014, **136**, 8654
38 Y. Zhang, B. Li, R. Krishna, Z. Wu, D. Ma, Z. Shi, S. Ma, et al. *Chem. Commun.*, 2015, **51**, 2714
39 Y. Wang, Z. Hu, Y. Cheng, D. Zhao, *Ind. Eng. Chem. Res.* 2017, **56**, 4508
40 U. Böhme, B. Barth, C. Paula, A. Kuhnt, W. Schwieger, J. Caro, M. Hartmann, *Langmuir.*, 2013, **29**, 8592
41 W. Liang, F. Xu, X. Zhou, J. Xiao, Q. Xia, Y. Li, Z. Li, *Chem. Eng. Sci.*, 2016, **148**, 275
42 P. -Q. Liao, W.-X. Zhang, J.-P. Zhang, X.-M. Chen, *Nat. Commun.*, 2015, **6**, 8697
43 Y. Chen, Z. Qiao, H. Wu, D. Lv, R. Shi, Q. Xia, J. Zhou, Z. Li, *Chem. Eng. Sci.*, 2018, **175**, 110
44 R.-B. Lin, H. Wu, W. Zhou, B. Chen, *J. Am. Chem. Soc.*, 2018, **140**, 12940
45 L. Li, R. –B. Lin, R. Krishna, H. Li, J. Li, B. Chen et al., *Science*, 2018, **362**, 443
46 Y. Wu, H. Chen, D. Liu, Y. Qian, H. Xi, *Chem. Eng. Sci.*, 2015, **124**, 144
47 N. Nijem, J.-F. Veyan, L. Kong, K. Li, J. Li, D. Langreth, Y. J. Chabal et al, *J. Am, Chem. Soc.*, 2010, **132**, 1654
48 K. Tan, N. Nijem, P. Canepa, Q. Gong, J. Li, T. Thonhauser, Y. J. Chabal, *Chem. Mater.*, 2012, **24**, 3153
49 A. Hijazi, J. C. Kemmegne–Mbouguen, E. Cadot, etc., *Dalton Trans.*, 2013, **42**, 4848
50 J. Y. Lee, D. H. Olson, L. Pan, T. J. Emge, J. Li, *Adv. Funct. Mater.*, 2007, **17**, 1255
51 N. Nijem, J. –F. Veyan, L. Kong, J. Li, Y. J. Chabal et al., *J. Am. Chem. Soc.*, 2010, **132**, 1654
52 K. Tan, P. Canepa, J. Liu, D. H. Johnson, J. Li, Y. J. Chabal et al., *Chem. Mater.*, 2013, **25**, 4653
53 J. Pires, M. L. Pinto, V. K. Saini, *ACS Appl. Mater. Interfaces.*, 2014, **6**, 12093
54 Q. M. Wang, D. Shen, M. Bülow, M. L. Lau, S. Deng, F. R. Fitch, N. O. Lemcoff, J. Semanscin, *Micropor. Mesopor. Mat.*, 2002, **55**, 217
55 S. Yang, A. J. Ramirez-Cuesta, R. Newby, V. Garcia-Sakai, P. Manuel, M. Schröder, etc. Nat. Chem., 2015, 7, 121.